Accepted Manuscript

Discovery of Enantioselectivity of Urea Inhibitors of Soluble Epoxide Hydrolase

Manoj Manickam, Thanigaimalai Pillaiyar, PullaReddy Boggu, Eeda Venkateswararao, Hitesh B. Jalani, Nam-Doo Kim, Seul Ki Lee, Jang Su Jeon, Sang Kyum Kim, Sang-Hun Jung

Graphical Abstract

Discovery of Enantioselectivity of Urea Inhibitors of Soluble Epoxide Hydrolase
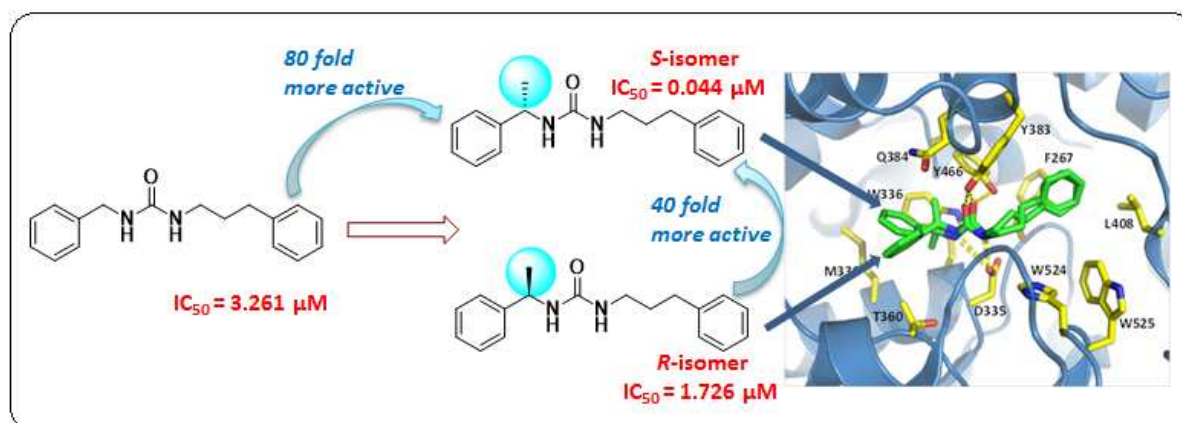
Discovery of Enantioselectivity of Urea Inhibitors of Soluble Epoxide Hydrolase

Manoj Manickam[a], Thanigaimalai Pillaiyar[a], PullaReddy Boggu[a], Eeda Venkateswararao[a], Hitesh B. Jalani[a], Nam-Doo Kim[b], Seul Ki Lee[a], Jang Su Jeon[a], Sang Kyum Kim[a], Sang-Hun Jung[a]*

[a]College of Pharmacy and Institute of Drug Research and Development, Chungnam National University, Daejeon 34134, Korea

[b]DGMIF, New Drug Development Center, 80, Cheombok-ro, Dong-gu, Daegu, Korea, 41061

Abstract

Soluble epoxide hydrolase (sEH) hydrolyzes epoxyeicosatrienoic acids (EETs) in the metabolic pathway of arachidonic acid and has been considered as an important therapeutic target for chronic diseases such as hypertension, diabetes and inflammation. Although many urea derivatives are known as sEH inhibitors, the enantioselectivity of the inhibitors is not highlighted in spite of the stereoselective hydrolysis of EETs by sEH. In an effort to explore the importance of enantioselectivity in the urea scaffold, a series of enantiomers with the stereocenter adjacent to the urea nitrogen atom were prepared. The selectivity of enantiomers of 1-(α-alkyl-α-phenylmethyl)-3-(3-phenylpropyl)ureas showed wide range differences up to 125 fold with the low IC_{50} value up to 13 nM. The *S*-configuration with planar phenyl and small alkyl groups at α-position is crucial for the activity and selectivity. However, restriction of the free rotation of two α-groups with indan-1-yl or 1,2,3,4-tetrahydronaphthalen-1-yl moiety abolishes the selectivity between the enantiomers, despite the increase in activity up to 13 nM. The hydrophilic group like sulfonamido group at *para* position of 3-phenylpropyl motif of 1-(α-alkyl-α-phenylmethyl-3-(3-phenylpropyl)urea improves the activity as well as enantiomeric selectivity. All these ureas are proved to be specific inhibitor of sEH without inhibition against mEH.

*Corresponding author: jungshh@cnu.ac.kr. Tel.; +82 42 821 5939; Fax +82 42 823 6566;
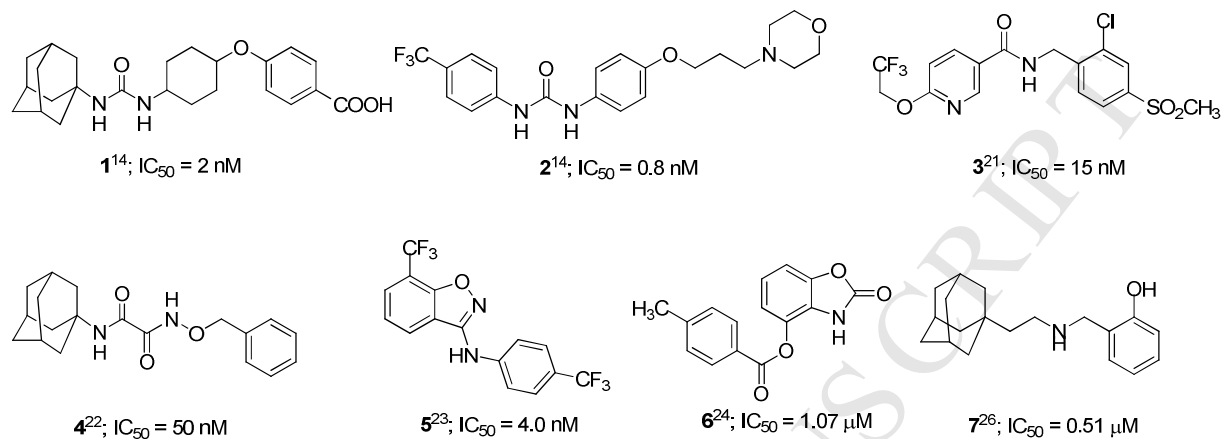
Present address: College of Pharmacy and Institute of Drug Research and development,

Chungnam National University, Daejeon 34134, Korea

1. Introduction

In humans, soluble epoxide hydrolase (sEH) plays an important role in the metabolism of endogenous chemical mediators such as epoxides of arachidonic acid [1], linoleic acid [2] and other lipids [3]. sEH hydrolyzes epoxides of arachidonic acid (epoxyeicosatrienoic acids, EETs) to the corresponding diols (dihydroxyeicosatrienoic acids, DHETs) [4]. EETs are known as effective modulators of blood pressure and inflammation [4]. The cardiovascular protective actions of sEH inhibitors were first described in animal models of hypertension in 2000 [5,6]. Since then the evidences have been accumulated to demonstrate that sEH inhibitors lower blood pressure in several animal models of hypertension, such as spontaneously hypertensive rats as well as angiotensin II-induced hypertensive models [7-9]. In these regards, the sEH enzyme has gained considerable attention as a therapeutic target for cardiovascular diseases over the last few years [10-13] and thus the inhibition of sEH provides the novel strategy for the treatment of hypertension and vascular inflammation [5-7,14].

In addition, the sEH enzyme regulates many other metabolic pathways and thus the inhibitors display anti-fibrotic [15], anti-platelet aggregation properties [16,17], and could be an alternative to treat diabetic neuropathy [18] and inflammation-induced carcinogenesis [19,20]. Therefore, these also prove sEH as a potentially important pharmaceutical target. Several groups have

reported the synthesis and evaluation of sEH inhibitors with diverse pharmacophoric scaffolds with potency varying from nanomolar to micromolar ranges (Fig. 1) [14, 21-26].

1[14]; IC_{50} = 2 nM

2[14]; IC_{50} = 0.8 nM

3[21]; IC_{50} = 15 nM

4[22]; IC_{50} = 50 nM

5[23]; IC_{50} = 4.0 nM

6[24]; IC_{50} = 1.07 μM

7[26]; IC_{50} = 0.51 μM

Figure 1. Representative examples of sEH inhibitors

Among them, the 1,3-disubstituted ureas are the most potent pharmacophore for the inhibition of sEH [27-30]. The binding mode (Fig. 2) of urea pharmacophore with human sEH was determined by X-ray crystallography and mimics the transition state of epoxide ring opening catalyzed by the enzyme (Fig. 2A), which shows the formation of tight hydrogen bonds with the active site residue Asp333 as shown in Fig. 2B. [31-33].
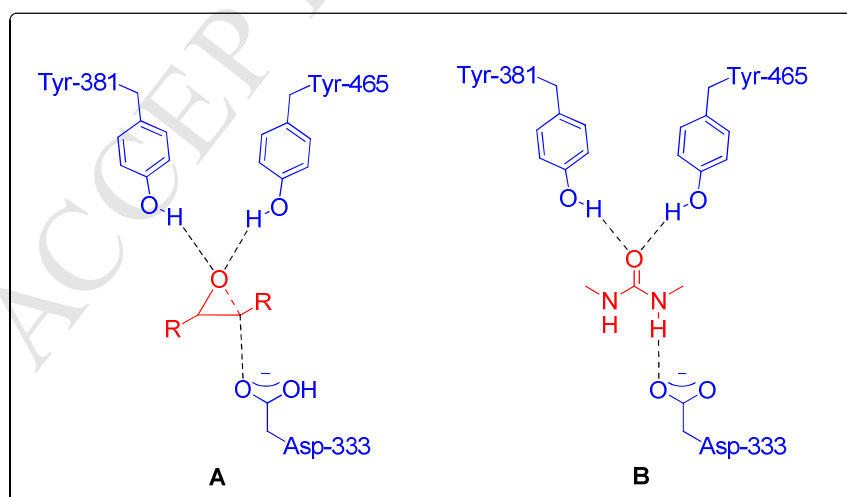
Figure 2. A) Transition state of epoxide ring opening catalyzed by sEH, B) Binding mode of urea which mimic the transition state[31]

Hydrolysis of epoxides or EETs by sEH showed diverse features depending on structures of substrates. The sEH catalyzed hydrolysis of substituted racemic epoxides gives a mixture of unreacted epoxides and the corresponding diols as shown in Fig. 3 [34]. For example, the methyl and butyl substituent in the racemic epoxide gives 16 % ee of unreacted 2*R*,3*S* epoxide and 10 % ee of the 2*R*,3*R* diol, whereas the hydroxyethyl and pentyl substituted epoxide gives >98 % ee of unreacted 3*R*,4*S* epoxide and >98 % of 2*R*,3*R* diol, which demonstrate that the sEH allow stereoselective ring opening of the epoxide and the stereochemistry of the products depends upon the substitution pattern on the epoxide ring (Fig. 3A). The arachidonic acid metabolism by CYP450 gives four regio isomers namely 5,6-EET, 8,9-EET, 11,12-EET and 14,15-EET, each having a mixture of *S*/*R*- and *R*/*S*-enantiomers with different ratio. Among the regio isomers, the 14,15-EET is the most preferred substrate for the hydrolysis catalyzed by sEH, whereas the 5,6-EET is the least preferred one. The 8,9-EET and 11,12-EET being the moderately preferred substrates [35]. The sEH catalyzed enantioselective hydrolysis of 14(*R*),15(*S*)-EET on rabbit liver or lung cytosol gives 82 % 14(*R*),15(*R*) diol whereas the same hydrolysis of 14(*S*),15(*R*)-EET gives only 35 % 14(*R*),15(*R*) diol, which also illustrate that stereochemistry of substrate influences the formation of stereoisomers of diol products (Fig. 3B). Moreover the hydration rate of 14(*R*),15(*S*)-EET (7994 nmol/mg protein/min) is four times faster than that of 14(*S*),15(*R*)-EET (1992 nmol/mg protein/min) [35].
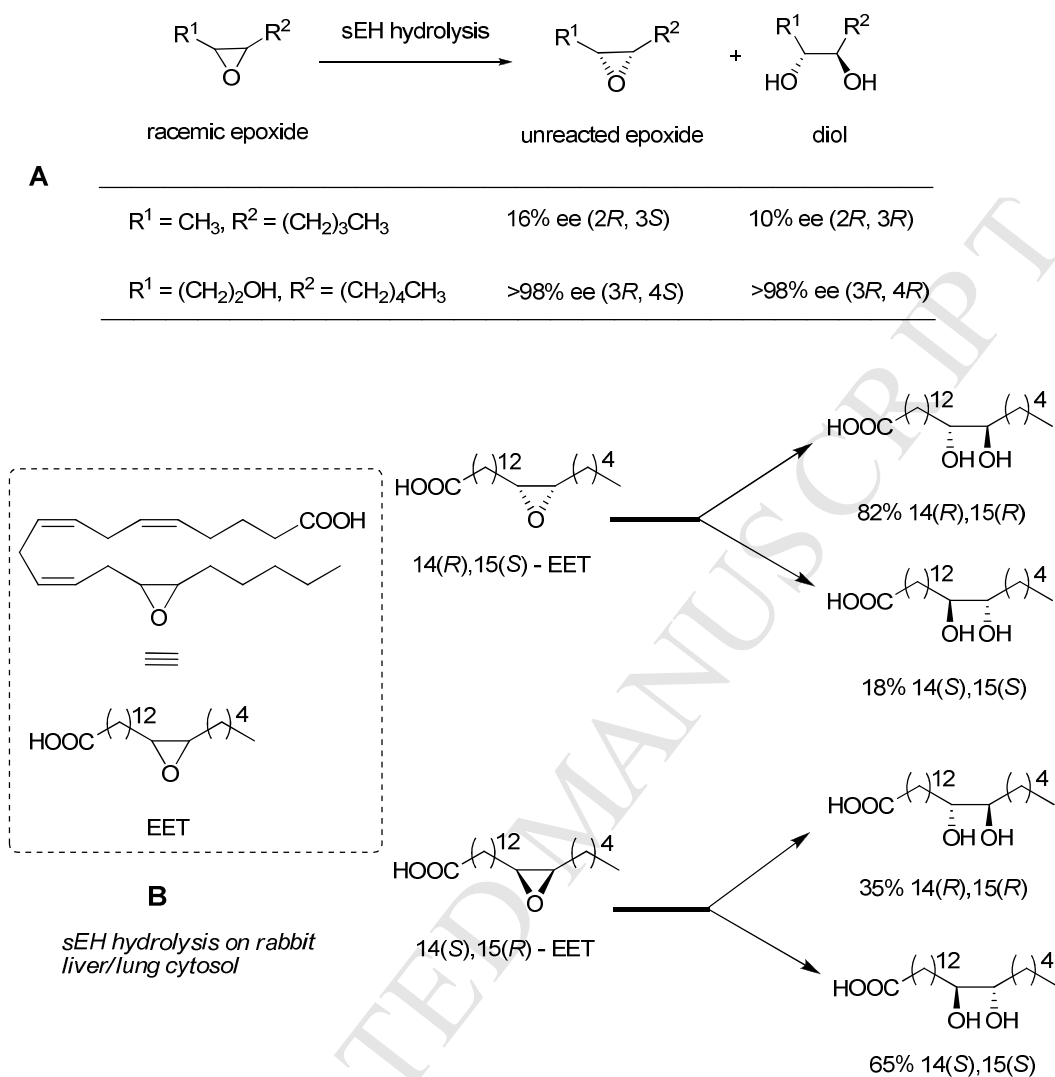
Figure 3. A) Stereoselective hydrolysis of epoxides by sEH, B) Stereoselective hydrolysis of EET by sEH

All the above points confirm that stereochemistry and substituents of epoxide ring influence the rate and the ratio of formation of the stereoisomers of the diol products by sEH. Therefore we inferred that stereoisomers of sEH inhibitor might differentiate the inhibitory activity and

accordingly investigated the possibility of different inhibitory activity of enantiomers of di(phenylalkyl)urea scaffold containing a stereocenter at α-position as shown in Fig. 4.
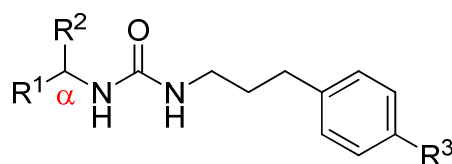
**Figure 4**. Designed urea **8**

2. Chemistry

The urea derivatives **8a-j** were prepared by the reaction of optical isomers of amines **9** (commercially available) and 3-phenylpropyl isocyanate **10** (Scheme 1) in high yields (80 - 90 %). Ureas **8k(S)** and **8k(R)** with sulfonamide substitution were prepared as illustrated in Scheme 2. Protection of 3-phenylpropylamine **11** was initially conducted with trifluoroacetic anhydride to give **12**. The following chlorosulfonation reaction of **12** generated **13**, which was converted by the treatment with ammonia gas to sulfonamide **14**. Deprotection of **14** by the reaction with K_2CO_3 in methanol/water gave sulfamoyl substituted amine **15** which was used for the preparation of ureas **8k(S)** and **8k(R).** The *R*- or *S*- isomer of 1-phenylethylamine was treated with triphosgene in the presence of *N,N*-diisopropylethylamine for 0.5 h followed by the addition of the sulfamoyl substituted amine **15** to obtain the ureas **8k(S)** and **8k(R).**
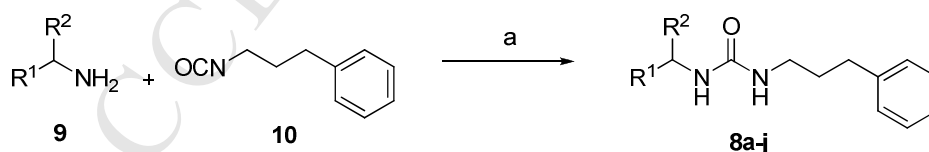
Scheme 1. Synthesis of urea derivatives **8a-j**

Reagents and conditions: a) acetonitrile, RT, 8 h
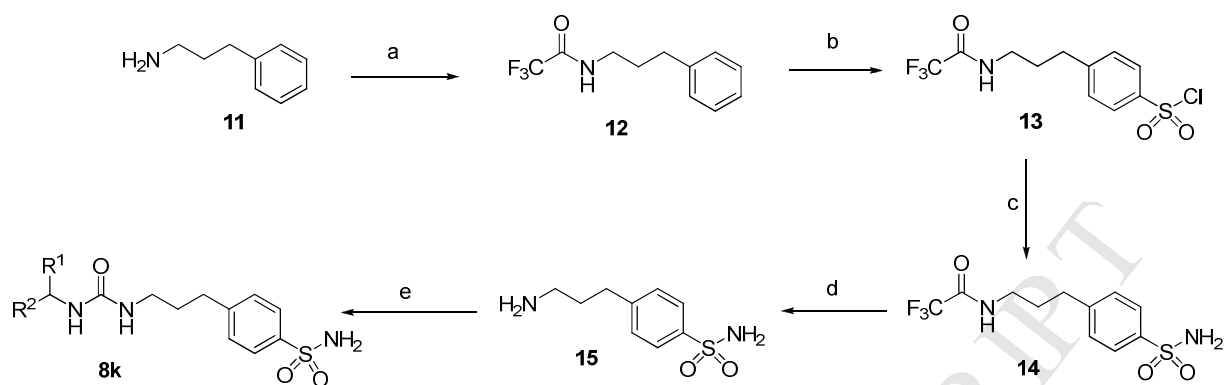
Scheme 2. Synthesis of sulfonamide substituted ureas **8k(*S*)** and **8k(*R*).**

Reagents and conditions: a) $(CF_3CO)_2O$, TEA, MC, 3 h; b) $ClSO_3H$, MC, 0 °C-RT, 3 h; c) NH_3 gas, 0.5 h; d) K_2CO_3, MeOH/H_2O, 10 h; e) (*R*)- or (*S*)-1-phenylethylamine, triphosgene, DIPEA, THF, 0 °C-RT, 8 h
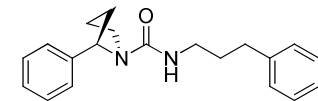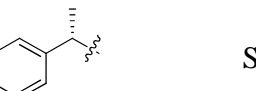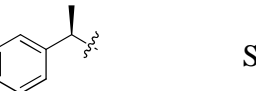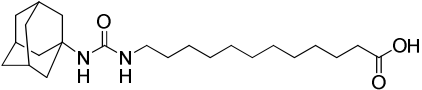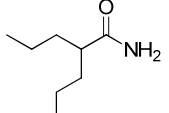
3. Results and Discussion

The *in vitro* sEH inhibition activity was determined using 14,15-EET as a substrate and the results are summarized in Table 1. The assay results for the inhibition of mEH enzyme are also included in Table 1. The assay protocols are described in the experimental section.

Table 1. Synthesized compounds **8** with sEH and mEH inhibitory activity

Comp. No. (configuration)	R^1 R^2	R^3	sEH inhibition IC$_{50}$ (uM)	mEH activity at 10 uM (%)
8a		H	3.26 (2.53 to 4.20) [†]	105 ± 0.8

8b(S)		H	0.044 (0.037 to 0.051) [†]	84.6 ± 0.7
8b(R)		H	1.73 (1.44 to 2.07) [†]	102 ± 0.0
8c(S)		H	19.99 (8.69 to 45.98) [†]	107 ± 0.8
8c(R)		H	2.74 (2.05 to 3.66) [†]	102 ± 3.7
8d(S)		H	0.182 (0.151 to 0.219) [†]	99.4 ± 2.3
8d(R)		H	0.302 (0.196 to 0.465) [†]	103 ± 0.0
8e(S)		H	0.036 (0.022 to 0.057) [†]	106 ± 2.7
8e(R)		H	4.50 (3.26 to 6.21) [†]	103 ± 1.5
8f(S)		H	0.043 (0.034 to 0.054) [†]	102 ± 1.1
8f(R)		H	0.364 (0.327 to 0.404) [†]	98.7 ± 2.2
8g(S)		H	0.065 (0.051 to 0.083) [†]	112 ± 6.9
8g(R)		H	0.022 (0.017 to 0.028) [†]	110 ± 3.5
8h(S)		H	0.013 (0.010 to 0.016) [†]	106 ± 0.9
8h(R)		H	0.013 (0.010 to 0.017) [†]	106 ± 0.3
8i(S)			0.332 (0.253 to 0.428) [†]	99.8 ± 1.2

8i(R)			1.51 (1.15 to 1.98) †	101 ± 0.2
8j(S)		H	0.063 (0.055 to 0.072) †	101 ± 1.6
8j(RS)		H	0.650 (0.053 to 0.797) †	102 ± 0.5
8k(S)		SO$_2$NH$_2$	0.022 (0.019 to 0.025) †	99.9 ± 4.2
8k(R)		SO$_2$NH$_2$	2.03 (1.57 to 2.63) †	101 ± 1.1
AUDA			0.059 (0.042 to 0.083)	N.D.
Valpromide			N.D.	50.9 ± 3.7

† indicates 95% confidence interval of the IC$_{50}$. mEH activity is expressed as the percentage of activity, relative to a control samples containing no inhibitor (100%).

Initially the inhibitory activity (IC$_{50}$ = 3.26 μM) of 1-benzyl-3-(3-phenylpropyl)urea (**8a**) against sEH was discovered in our laboratory. Compound **8a** is linear type of 1,3-dialkylsubstituted urea and thus ideal for the introduction of stereocenter at benzylic position (α-position) for the examination of selective inhibition of enantiomers of urea analogs. The introduction of methyl substituent at α-position showed a good enantioselectivity. The (*S*)-1-(1-phenylethyl)-3-(3-phenylpropyl)urea (**8b(S)**, IC$_{50}$ = 0.044 μM) showed 80 fold more potent than the parent benzyl analog **8a** and 40 fold more active than its *R*-isomer **8b(R)** (IC$_{50}$ = 1.73 μM). As shown in Fig. 5, the molecular docking analysis suggests that, compared to the parent benzyl analog **8a**, the α-methyl substituent of the **8b(S)** provide additional hydrophobic interaction to Try336, thus 80 fold more active. This additional binding increases the activity.
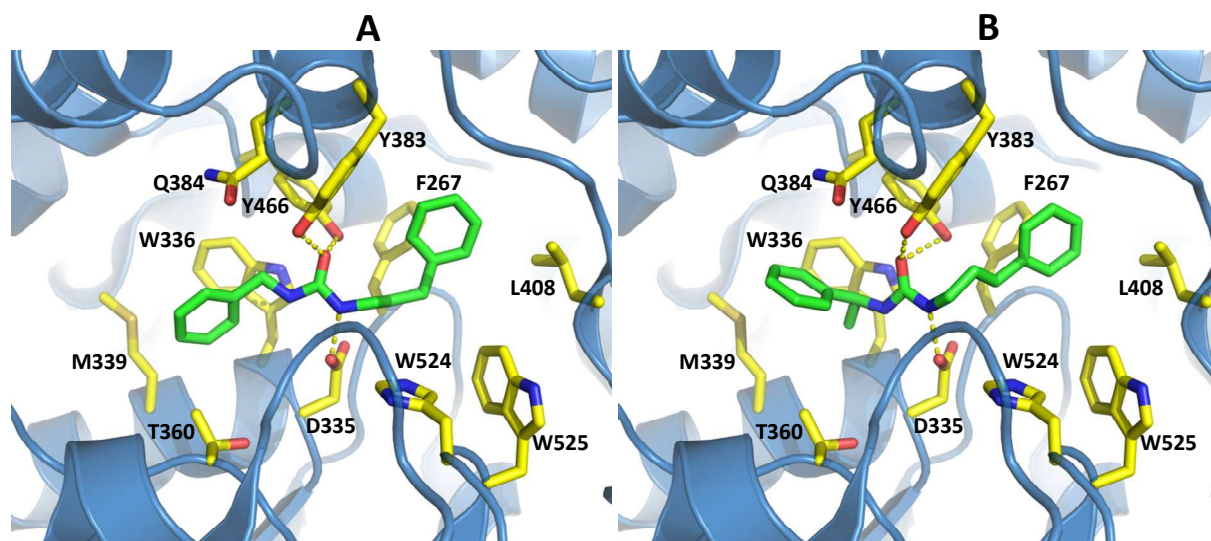
Figure 5. Binding model prediction data of **A**) compound **8a**, **B**) compound **8b(S)**. The yellow dashed line denoted hydrogen bond interactions.

In the docking model of the enantiomers **8b(S)** and **8b(R)** to sEH, the *α*-methyl substituent of the **8b(R)** is located to Glu384 (Fig. 6B) whereas the same of the *S*-isomer **8b(S)** is located to Try336 (Fig. 6A) and therefore experiences the stronger hydrophobic interaction, which results in 40 fold stronger activity.
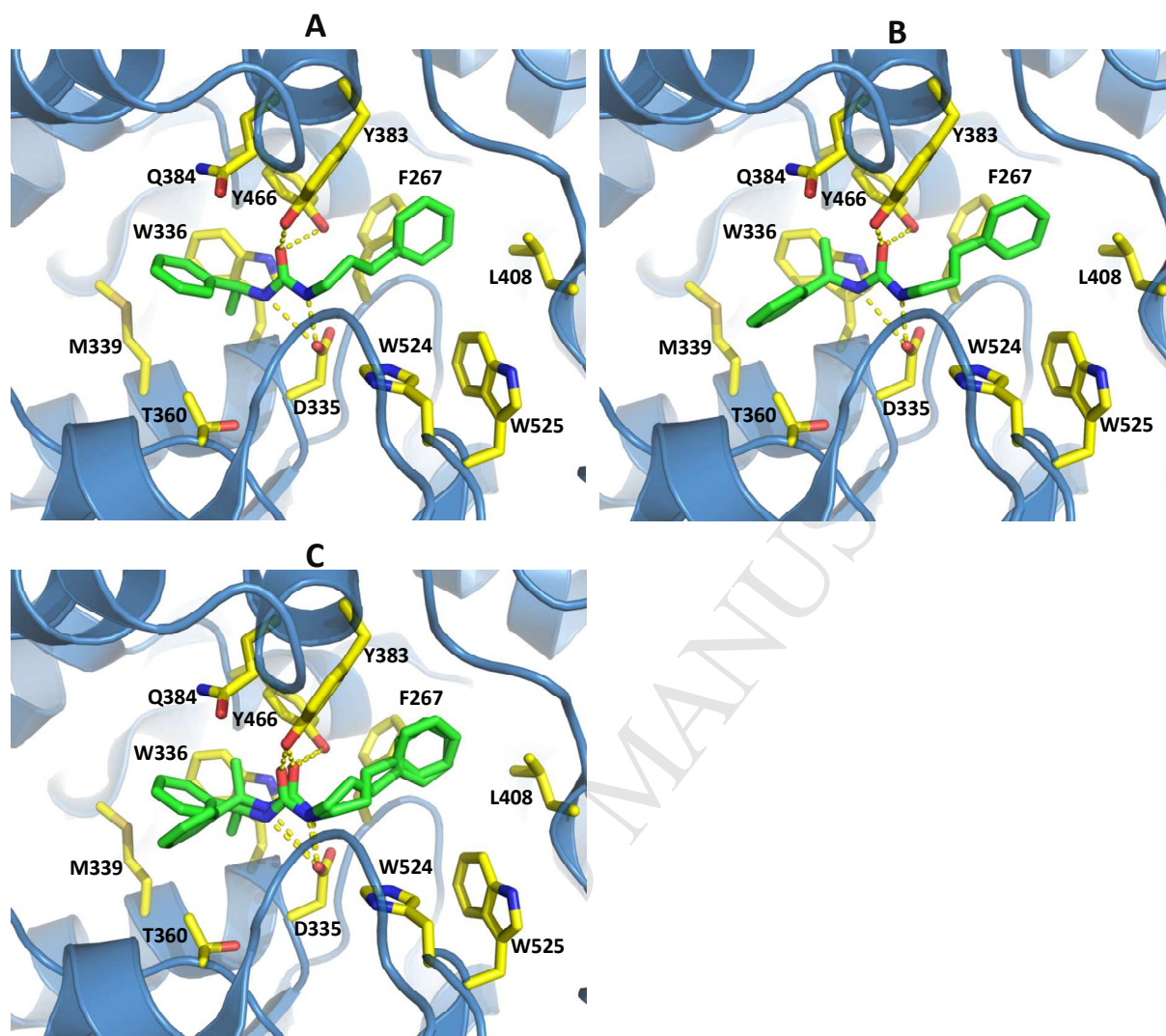
Figure 6. Binding model prediction data of **A**) **8b(*S*)**, **B**) **8b(*R*)**, **C**) Overlay of the predicted docking model of **8b(*S*)** and **8b(*R*)**. The yellow dashed line denoted hydrogen bond interactions.

Encouraged by these results, our next effort was to introduce additional hydrogen bonding property (HBA and HBD). Therefore, we introduced hydroxymethyl function at the *α*-position as shown in **8c(*S*)** and **8c(*R*)**. Unfortunately this additional hydrogen bonding function reduced the inhibitory activity compared to **8b(*S*)**. However, the *R*-isomer **8c(*R*)** (IC$_{50}$ = 2.74 μM) showed 10 fold more active than its *S*-isomer (**8c(*S*)**, IC$_{50}$ = 19.99 μM). Although **8c(*R*)** is designated as *R*-

isomer because of priority rule, the absolute configuration of **8c(*R*)** is the same as that of **8b(*S*)**. These results indicated that the absolute configuration at the *α*-position as shown in **8b(*S*)** is important for the selectivity between the enantiomers of these urea scaffolds in their inhibition of sEH.

In order to find the importance of phenyl ring at *α*-position of **8b**, it was changed to cyclohexyl ring which decreased the selectivity as well as activity. **8d(*S*)** (IC$_{50}$ = 0.182 μM) showed only 1.5 fold more activity compared to **8d(*R*)** (IC$_{50}$ = 0.302 μM). From the binding model prediction data, it is evident that, despite the phenyl and cyclohexyl rings are oriented towards the Met339, the planar phenyl group of **8b(*S*)** can bind more stably when compared to the bulky cyclohexyl group of **8d(*S*)** (Fig. 7).
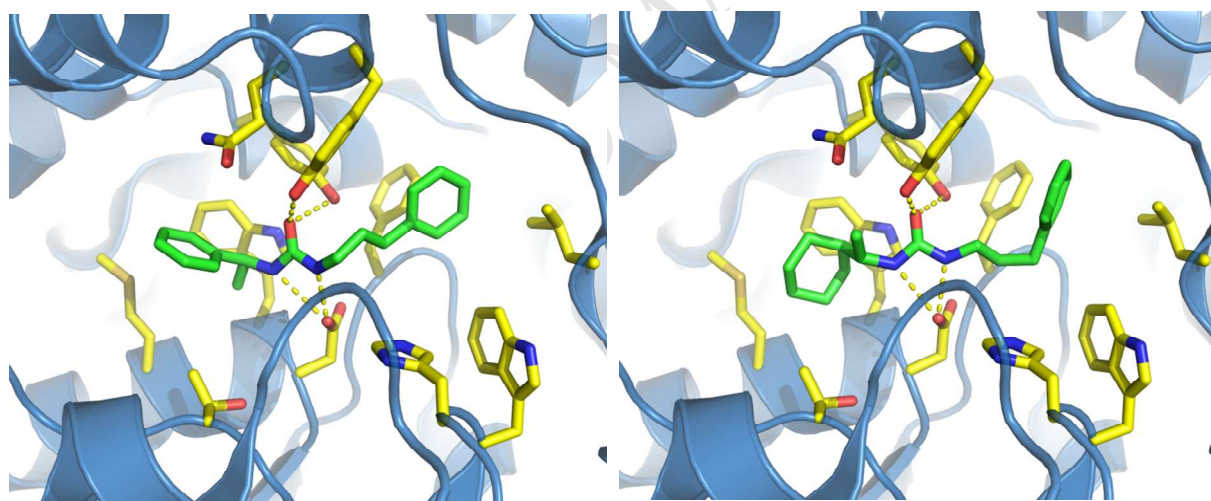
Figure 7. Binding model prediction data of **A**) compound **8b(*S*)**, **B**) compound **8d(*S*).** The yellow dashed line denoted hydrogen bond interactions.

In the next set of experiment, we focused on identification of the optimum size of the two groups at the *α*-position. To determine the effect of increment of size of alkyl function at *α*-position,

methyl group of **8b** was changed to ethyl as shown in **8e**. The *S*-isomer **8e(S)** (IC$_{50}$ = 0.036 μM) showed the 125 fold more potent activity than its *R*-isomer **8e(R)** (IC$_{50}$ = 4.50 μM) and the enhanced activity compared to **8b(S)**. These results indicated that the increase in size of alkyl function at α-position form methyl group to ethyl group improved the selectivity as well as the activity of *S*-isomer. However, the increase in the size of the phenyl group with naphthyl ring displayed a poor selectivity, though retained the activity as shown in **8f(S)** (IC$_{50}$ = 0.043 μM) and **8f(R)** (IC$_{50}$ = 0.364 μM). Thus the phenyl group is the optimum size for this position.

Next, to restrict the free rotation between the two α-groups, the α-group and the phenyl ring were rigidified with indan-1-yl or 1,2,3,4-tetrahydronaphthalen-1-yl moiety as shown in **8g** and **8h**. Surprisingly, the *S*-isomer **8g(S)** (IC$_{50}$ = 0.065 μM) of the indan-1-yl analog showed 3 times less activity compared to its *R*-isomer **8g(R)** (IC$_{50}$ = 0.022 μM) whereas the *S*-isomer of the tetrahydronaphthalen-1-yl analog **8h(S)** (IC$_{50}$ = 0.013 μM) showed nil activity difference compared to its *R*-isomer **8h(R)** (IC$_{50}$ = 0.013 μM). These results demonstrated that the rigidification of the α-position and the phenyl ring abolished the selectivity of these enantiomers for the inhibition of sEH. Unlike open chain analogs such as **8b(R)** or **8e(R)**, the activity of *R*-isomer **8h(R)** was remarkably enhanced to the activity level of its *S*-isomer **8h(S)**. The reason for the tetrahydronaphthalen-1-yl analog to show nil selectivity between the enantiomers can be explained from the molecular docking analysis as the binding mode of the two enantiomers is quite similar unlike the open chain isomers (Fig.8). On the other hand, the rigidification of the α-position and the urea nitrogen as shown in **8i** also demonstrated poor selectivity and weak activity. The *S*-isomer **8i(S)** (IC$_{50}$ = 0.332 μM) showed only 5 fold increase in activity compared to its *R*-isomer **8i(R)** (IC$_{50}$ = 1.51 μM). These above results suggest that the rigidification on either side of the α-position has no advantage for the selectivity.
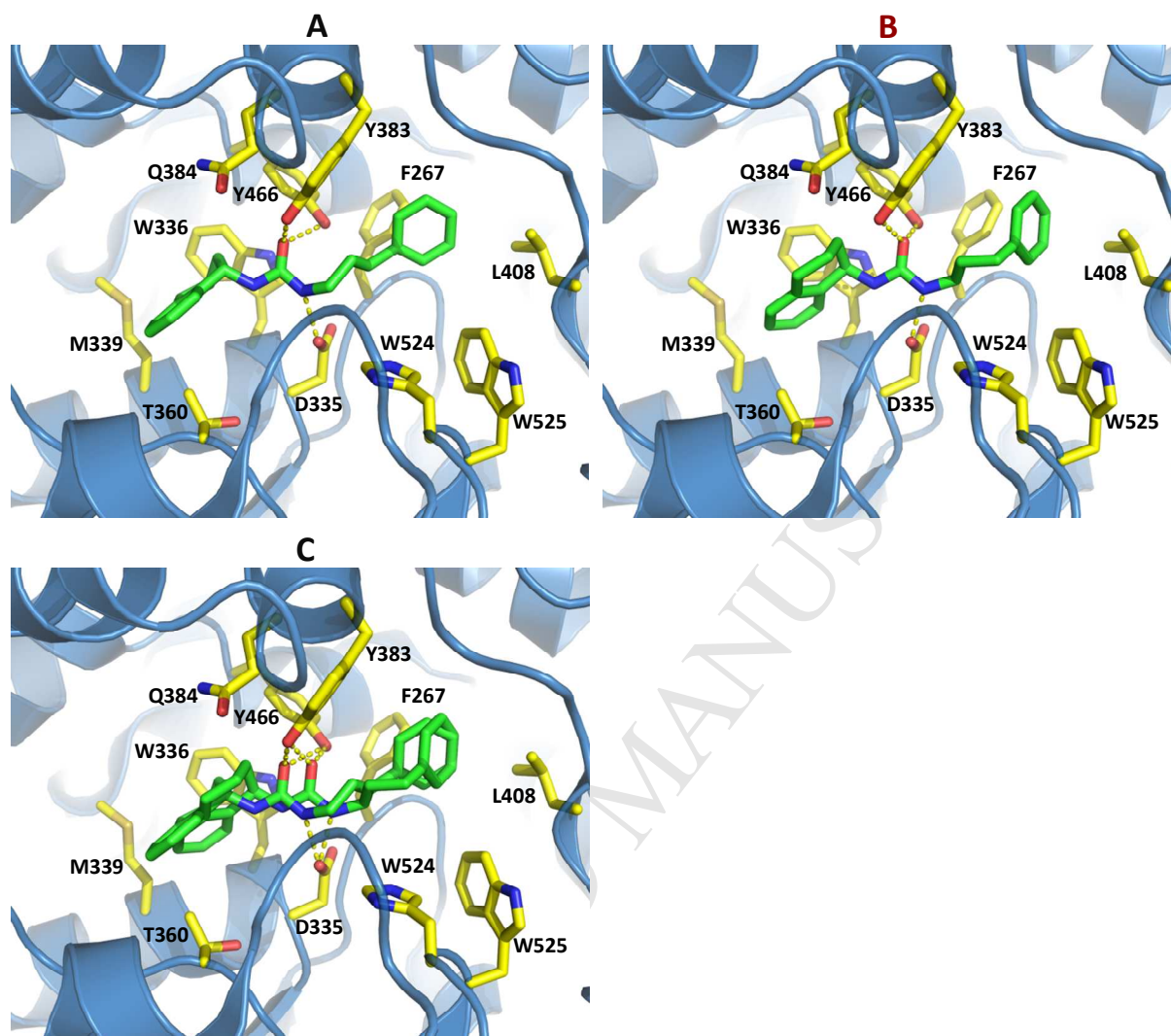
Figure 8. Binding model prediction of the six membered bicyclic enantiomers **A**) **8h(*S*)**, **B**) **8h(*R*)**, C) Overlay of the predicted docking model of **8h(*S*)** and **8h(*R*)**.

Next objective of our work was to study the effect of two small alkyl *α*-groups. Accordingly, the methyl and ethyl substituents at the *α*-position were introduced as shown in compounds **8j(*S*)** and **8j(*RS*)**. The *S*-isomer **8j(*S*)** (IC$_{50}$ = 0.063 μM) showed nearly the same level of activity as **8b(*S*)** and 20 fold more activity when compared to the *R*-isomer **8j(*R*)** (IC$_{50}$ = 1.24 μM: calculated from the IC$_{50}$ of *S*-isomer **8j(*S*)** and IC$_{50}$ (0.650 μM) of the racemic compound

8j(*RS*)). Although enantiomeric selectivity of *S*-isomer **8j(*S*) was reduced, these results opened the high possibility of replacement of phenyl of **8b(*S*)** with unbranched alkyl group for improvement of the selectivity as well as the activity.

Finally, to improve the water solubility, the hydrophilic sulfonamido group was introduced on the *para* position of phenyl group on propyl linkage of **8b** as shown in **8k**. The *S*-isomer **8k(*S*)** (IC$_{50}$ = 0.022 μM) showed 100 fold more activity compared to the *R*-isomer **8k(*R*)** (IC$_{50}$ = 2.03 μM) and more potent activity than **8b(*S*)**. Thus hydrophilic group enhanced the selectivity as well as the activity.

Since microsomal epoxide hydrolase (mEH) located in liver is essential for metabolic process, the selective inhibitor for sEH is necessary for the development. Thus the inhibitory effect of all compounds **8** against mEH were measured as shown in Table 1 and showed no activity at 10 μM. Therefore urea analogs **8** were proved as the specific inhibitors for sEH.
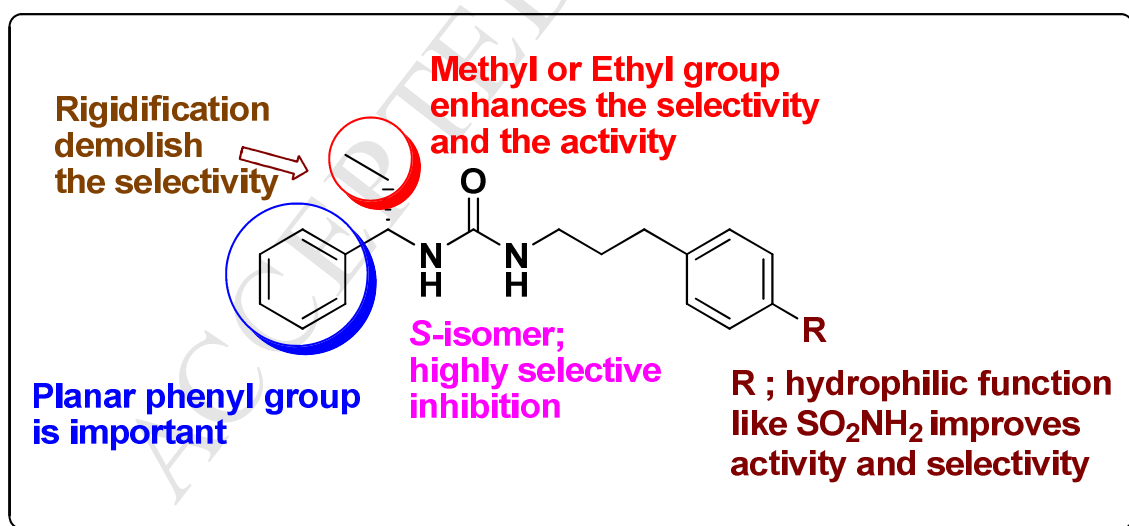
Figure 9. SAR analysis of the novel urea derivatives

4. Conclusion

In conclusion, the enantioselectivity in urea scaffold for the inhibition of sEH was first time investigated. Structure activity relationship study of the enantiomers demonstrated that the absolute configuration of the 1-(*α*-alkyl-*α*-phenylmethyl)-3-(3-phenylpropyl)urea scaffold is crucial for the selectivity as well as activity. The structure activity relationship is depicted in Figure 9. The selectivity of enantiomers of ureas **8** showed a wide range difference up to 125 fold with the low IC$_{50}$ value up to 13 nM. The *S*-configuration with planar phenyl and small alkyl groups at *α*-position of 1-(*α*-alkyl-*α*-phenylmethyl)-3-(3-phenylpropyl)urea is crucial for the activity and selectivity. However, restriction of the free rotation of two *α*-groups with indan-1-yl or 1,2,3,4-tetrahydronaphthalen-1-yl moiety abolishes the selectivity between the enantiomers, despite the increase in activity of **8h(*S*)** and **8h(*R*)** up to 13 nM. The hydrophilic function like sulfonamido group at *para* position of 3-phenylpropyl of 1-(*α*-alkyl-*α*-phenylmethyl-3-(3-phenylpropyl)urea increases the activity as well as enantiomeric selectivity. All the synthesized ureas **8** were proved to be specific inhibitors of sEH without inhibition against mEH. Therefore the selectivity of the sEH inhibition between the two enantiomers of 1-(*α*-alkyl-*α*-phenylmethyl-3-(3-phenylpropyl)urea provides new structural insights toward the binding site of soluble epoxide hydrolase that will lead to the discovery of novel and potent inhibitors.

5. Experimental section

5.1 Chemistry

Melting points were determined on Electro thermal 1A 9100 MK2 apparatus and are uncorrected. All commercial chemicals were used as obtained and all solvents were purified by the standard procedures [36] prior to use. All the chiral amines purchased were optically pure (>98 % ee). Thin layer chromatography was performed on E Merck silica gel GF-254 pre-coated

plates and the identification was done with UV light and colorization with spray 10 % phosphomolybdic acid followed by heating. Flash column chromatography was performed with E Merck silica gel (230-400 mesh). Infrared spectrum was recorded by using sample as such on FT-IR spectrum with Nicolet-380 models. NMR spectra were measured against the peak of tetramethylsilane by JEOL, JNM-AL-400 (Alice) 400 FT-NMR spectrometer. High resolution mass spectra (HRMS) were measured in ESI ionization using AB Sciex TripleTOF 5600 LCMS instrument.

*5.1.1. General synthetic procedure for the preparation of urea derivatives **8a-j**:* To the corresponding amine **9** (0.710 mmol) in acetonitrile (5 mL), 3-phenylpropyl isocyanate **10** (0.645 mmol) was added and allowed to stir for 8 h at ambient temperature. The resulting mixture was portioned between water and ethyl acetate. The organic layer was dried over anhydrous Na_2SO_4 and evaporated under reduced pressure. The crude mixture was subjected to column chromatography to obtain the pure compounds.

*5.1.1.1. 1-Benzyl-3-(3-phenylpropyl)urea (**8a**).* Yield 89 %; White solid; mp 96-98 °C; IR (neat): 3308, 2868, 1620, 1559, 1494, 1453 cm^{-1}; ^{1}H-NMR (CDCl$_3$) δ 1.76-1.84 (m, 2H), 2.61 (t, J = 7.80 Hz, 2H), 3.17-3.21 (m, 2H), 4.33 (d, J = 6.00 Hz, 2H), 4.39 (bs, 1H), 4.66 (bs, 1H), 7.13-7.19 (m, 3H), 7.24-7.34 (m, 7H); ^{13}C-NMR (CDCl$_3$) δ 31.70, 33.02, 39.97, 44.36, 125.94, 127.28, 127.38, 128.38, 128.44, 128.84, 139.32, 141.62, 158.44; HRMS Calcd for $C_{17}H_{20}N_2O$ *m/z* [M+H] 269.1654, found 268.1682.

*5.1.1.2. (S)-1-(1-Phenylethyl)-3-(3-phenylpropyl)urea (**8b(S)**).* Yield 86 %; White solid; mp 78-80 °C; IR (neat): 3314, 3025, 2867, 1622, 1560, 1493, 1452 cm^{-1}; ^{1}H-NMR (CDCl$_3$) δ 1.42 (d, J = 7.20 Hz, 3H), 1.67-1.74 (m, 2H), 2.51 (t, J = 7.80 Hz, 2H), 3.06-3.18 (m, 2H), 4.44 (bs, 1H), 4.69-4.74 (m, 1H), 4.83 (d, J = 7.00 Hz, 1H), 7.07-7.34 (m, 10H); ^{13}C-NMR (CDCl$_3$) δ 23.51,

31.41, 32.90, 40.05, 50.81, 125.81, 125.95, 127.58, 128.32, 128.42, 128.90, 141.31, 143.57, 157.90; HRMS Calcd for $C_{18}H_{22}N_2O$ *m/z* [M+H] 283.1810, found 283.1840

5.1.1.3. (R)-1-(1-Phenylethyl)-3-(3-phenylpropyl)urea (8b(R)). Yield 88 %; White solid; mp 78-80 °C; IR (neat): 3314, 3025, 2869, 1622, 1560, 1493, 1452 cm^{-1}; ^{1}H-NMR (CDCl$_3$) δ 1.45 (d, *J* = 7.20 Hz, 3H), 1.70-1.78 (m, 2H), 2.51 (t, *J* = 7.80 Hz, 2H), 3.10-3.17 (m, 2H), 4.40-4.45 (bs, 1H), 4.64-4.71 (m, 1H), 4.83 (d, *J* = 7.00 Hz, 1H), 7.07-7.34 (m, 10H); ^{13}C-NMR (CDCl$_3$) δ 23.50, 31.35, 32.88, 40.10, 50.90, 125.81, 125.97, 127.66, 128.31, 128.43, 128.93, 141.25, 143.38, 157.92; HRMS Calcd for $C_{18}H_{22}N_2O$ *m/z* [M+H] 283.1810, found 283.1837

5.1.1.4. (S)-1-(2-Hydroxy-1-phenylethyl)-3-(3-phenylpropyl)urea (8c(S)). Yield 84 %; Pale white solid; mp 104-106 °C; IR (neat): 3415, 3310, 3021, 2924, 1625, 1563, 1489, 1450 cm^{-1}; ^{1}H-NMR (DMSO-*d$_6$*) δ 1.59-1.69 (m, 2H), 2.55 (t, *J* = 7.50 Hz, 2H), 2.94-3.01 (m, 2H), 3.52-3.57 (m, 2H), 4.62-4.69 (m, 1H), 4.85 (t, *J* = 7.20 Hz, 1H), 6.08 (t, *J* = 7.60 Hz, 1H), 6.30 (d, *J* = 7.80 Hz, 1H), 7.14-7.32 (m, 10H); ^{13}C-NMR (DMSO-*d$_6$*) δ 31.82, 32.45, 38.69, 55.21, 65.22, 125.67, 126.43, 126.72, 127.91, 128.25, 128.26, 141.79, 142.64, 157.66. HRMS Calcd for $C_{18}H_{22}N_2O_2$ *m/z* [M+H] 299.1760, found 299.1791

5.1.1.5. (R)-1-(2-Hydroxy-1-phenylethyl)-3-(3-phenylpropyl)urea (8c(R)). Yield 82 %; Pale white solid; mp 105-107 °C; IR (neat): 3415, 3312, 3021, 2924, 1625, 1561, 1489, 1450 cm^{-1}; ^{1}H-NMR (DMSO-*d$_6$*) δ 1.58-1.69 (m, 2H), 2.55 (t, *J* = 7.50 Hz, 2H), 2.95-3.02 (m, 2H), 3.52-3.57 (m, 2H), 4.62-4.68 (m, 1H), 4.85 (t, *J* = 7.20 Hz, 1H), 6.06-6.10 (m, 1H), 6.30 (d, *J* = 7.80 Hz, 1H), 7.14-7.32 (m, 10H); ^{13}C-NMR (DMSO-*d$_6$*) δ 31.82, 32.45, 38.69, 55.21, 65.22, 125.65, 126.42, 126.71, 127.90, 128.24, 128.25, 141.78, 142.63, 157.65; HRMS Calcd for $C_{18}H_{22}N_2O_2$ *m/z* [M+H] 299.1760, found 299.1790

*5.1.1.6. (S)-1-(1-Cyclohexylethyl)-3-(3-phenylpropyl)urea (**8d(S)**).* Yield 80 %; White solid; mp 106-108 °C; IR (neat): 3331, 3020, 2866, 1625, 1564, 1498, 1448 cm^{-1}; ^{1}H-NMR (300 MHz, CDCl$_3$) δ 0.91-1.02 (m, 2H), 1.06 (d, *J* = 6.80 Hz, 3H), 1.12-1.30 (m, 4H), 1.63-1.76 (m, 5H), 1.79-1.89 (m, 2H), 2.66 (t, *J* = 7.60 Hz, 2H), 3.19 (t, *J* = 7.20 Hz, 2H), 3.50-3.58 (m, 1H), 7.17-7.21 (m, 3H), 7.26-7.31 (m, 2H); ^{13}C-NMR (CDCl3) δ 18.31, 26.09, 26.31, 28.87, 31.53, 33.08, 40.22, 43.41, 50.82, 126.06, 128.43, 128.54, 141.49, 158.13. HRMS Calcd for C$_{18}$H$_{28}$N$_2$O *m/z* [M+H] 289.2280, found 289.2311

*5.1.1.7. (R)-1-(1-Cyclohexylethyl)-3-(3-phenylpropyl)urea (**8d(R)**).* Yield 82 %; White solid; mp 106-108 °C; IR (neat): 3330, 3020, 2866, 1625, 1563, 1498, 1448 cm^{-1}; ^{1}H-NMR (CDCl$_3$) δ 0.91-1.04 (m, 2H), 1.06 (d, *J* = 6.80 Hz, 3H), 1.10-1.29 (m, 4H), 1.64-1.67 (m, 2H), 1.72-1.75 (m, 3H), 1.81-1.88 (m, 2H), 2.66 (t, *J* = 7.60 Hz, 2H), 3.19 (t, *J* = 7.20 Hz, 2H), 3.52-3.55 (m, 1H), 7.17-7.21 (m, 3H), 7.27-7.31 (m, 2H); ^{13}C-NMR (CDCl$_3$) δ 18.32, 26.11, 26.33, 28.88, 31.55, 33.10, 40.24, 43.43, 50.84, 126.08, 128.45, 128.55, 141.50, 158.15; HRMS Calcd for C$_{18}$H$_{28}$N$_2$O *m/z* [M+H] 289.2280, found 289.2311

*5.1.1.8. (S)-1-(1-Phenylpropyl)-3-(3-phenylpropyl)urea (**8e(S)**).* Yield 85 %; White solid; mp 100-102 °C; IR (neat): 3318, 3019, 2878, 1621, 1565, 1492, 1451 cm^{-1}; ^{1}H-NMR (CDCl$_3$) δ 0.89 (t, *J* = 7.20 Hz, 3H), 1.66-1.74 (m, 2H), 1.75-1.80 (m, 2H), 2.48 (t, *J* = 7.50 Hz, 2H), 3.04-3.21 (m, 2H), 4.38 (t, *J* = 7.20 Hz, 1H), 4.56-4.97 (bs, 2H), 7.05-7.07 (m, 2H), 7.14-7.23 (m, 3H), 7.27-7.37 (m, 5H); ^{13}C-NMR (CDCl$_3$) δ 10.57, 30.48, 31.38, 32.87, 40.06, 57.07, 125.95, 126.36, 127.68, 128.31, 128.42, 128.86, 141.30, 142.18, 158.13; HRMS Calcd for C$_{19}$H$_{24}$N$_2$O *m/z* [M+H] 297.1967, found 297.1993

*5.1.1.9. (R)-1-(1-Phenylpropyl)-3-(3-phenylpropyl)urea (**8e(R)**).* Yield 80 %; White solid; mp 99-101 °C; IR (neat): 3320, 3019, 2880, 1621, 1566, 1492, 1451 cm^{-1}; ^{1}H-NMR (CDCl$_3$) δ 0.88

(t, J = 7.20 Hz, 3H), 1.67-1.73 (m, 2H), 1.74-1.80 (m, 2H), 2.48 (t, J = 7.50 Hz, 2H), 3.04-3.19 (m, 2H), 4.41 (t, J = 7.20 Hz, 1H), 4.60-5.20 (bs, 2H), 7.06-7.08 (m, 2H), 7.15-7.25 (m, 3H), 7.27-7.36 (m, 5H); ^{13}C-NMR (CDCl$_3$) δ 10.52, 30.43, 31.39, 32.81, 39.96, 56.98, 125.99, 126.41, 127.69, 128.37, 128.42, 128.86, 141.40, 142.32, 158.24; HRMS Calcd for C$_{19}$H$_{24}$N$_2$O m/z [M+H] 297.1967, found 297.1994

5.1.1.10. (S)-1-(-Naphthalen-1-yl)ethyl)-3-(3-phenylpropyl)urea (8f(S)). Yield 88 %; White powder; mp 137-139 °C; IR (neat): 3326, 3011, 2881, 1623, 1565, 1493, 1450 cm^{-1}; ^{1}H-NMR (CDCl$_3$) δ 1.61 (d, J = 6.90 Hz, 3H), 1.64-1.73 (m, 2H), 2.41-2.49 (m, 2H), 3.05-3.14 (m, 2H), 5.52-5.58 (m, 1H), 6.98-7.00 (m, 2H), 7.11-7.22 (m, 3H), 7.43-7.57 (m, 4H), 7.78 (d, J = 8.10 Hz, 1H), 7.88 (dd, J = 7.80 Hz, 1.80 Hz, 1H), 8.13 (d, J = 8.40 Hz, 1H); ^{13}C-NMR (CDCl$_3$) δ 22.33, 31.24, 32.73, 40.02, 46.94, 122.58, 122.76, 125.51, 125.92, 126.65, 128.24, 128.39, 128.42, 129.04, 129.05, 130.54, 134.01, 138.21, 141.11, 157.80; HRMS Calcd for C$_{22}$H$_{24}$N$_2$O m/z [M+H] 333.1967, found 333.2000

5.1.1.11. (R)-1-(Naphthalen-1-yl)ethyl)-3-(3-phenylpropyl)urea (8f(R)). Yield 86 %; White powder; mp 137-139 °C; IR (neat): 3325, 3010, 2886, 1623, 1561, 1495, 1450 cm^{-1}; ^{1}H-NMR (CDCl$_3$) δ 1.61 (d, J = 6.90 Hz, 3H), 1.64-1.71 (m, 2H), 2.41-2.47 (m, 2H), 3.03-3.11 (m, 2H), 4.72-4.90 (bs, 2H), 5.49-5.53 (m, 1H), 6.96-6.98 (m, 2H), 7.12-7.21 (m, 3H), 7.44-7.58 (m, 4H), 7.79 (d, J = 8.10 Hz, 1H), 7.89 (dd, J = 7.80 Hz, 1.80 Hz, 1H), 8.09 (d, J = 8.40 Hz, 1H); ^{13}C-NMR (CDCl$_3$) δ 22.29, 31.23, 32.68, 39.91, 46.77, 122.58, 122.84, 125.56, 125.96, 126.65, 128.31, 128.40, 128.43, 129.06, 129.07, 130.54, 134.03, 138.57, 141.24, 157.88; HRMS Calcd for C$_{22}$H$_{24}$N$_2$O m/z [M+H] 333.1967, found 333.1997

5.1.1.12. (S)-1-(2,3-Dihydro-1H-inden-1-yl)-3-(3-phenylpropyl)urea (8g(S)). Yield 85 %; White solid; mp 148-150 °C; IR (neat): 3310, 2936, 1620, 1571, 1523, 1454, 956 cm^{-1}; ^{1}H-NMR

(CDCl$_3$) δ 1.72-1.79 (m, 1H), 1.81-1.89 (m, 2H), 2.51-2.58 (m, 1H), 2.65 (t, J = 7.80 Hz, 2H), 2.78-2.86 (m, 1H), 2.91-2.98 (m, 1H), 3.20 (t, J = 7.20 Hz, 2H), 4.72-4.91 (bs, 2H), 5.21 (t, J = 7.60 Hz, 1H), 7.16-7.30 (m, 9H); ^{13}C-NMR (CDCl$_3$) δ 29.97, 31.36, 32.99, 34.37, 40.25, 55.91, 124.00, 124.88, 126.08, 126.81, 128.04, 128.40, 128.54, 141.32, 143.23, 143.21, 158.29; HRMS Calcd for C$_{19}$H$_{22}$N$_2$O m/z [M+H] 295.1810, found 295.1841

5.1.1.13. (R)-1-(2,3-Dihydro-1H-inden-1-yl)-3-(3-phenylpropyl)urea (8g(R)). Yield 86 %; White solid; mp 148-150 °C; IR (neat): 3312, 2936, 1620, 1571, 1523, 1455, 956 cm^{-1}; ^{1}H-NMR (300 MHz, CDCl$_3$) δ 1.72-1.79 (m, 1H), 1.81-1.88 (m, 2H), 2.50-2.58 (m, 1H), 2.65 (t, J = 7.80 Hz, 2H), 2.78-2.86 (m, 1H), 2.91-2.98 (m, 1H), 3.20 (t, J = 7.20 Hz, 2H), 4.40-4.50 (bs, 2H), 5.21 (t, J = 7.60 Hz, 1H), , 7.15-7.29 (m, 9H); ^{13}C-NMR (CDCl$_3$) δ 29.96, 31.32, 32.97, 34.33, 40.26, 55.93, 123.99, 124.88, 126.09, 126.82, 128.06, 128.40, 128.54, 141.29, 143.12, 143.21, 158.37; HRMS Calcd for C$_{19}$H$_{22}$N$_2$O m/z [M+H] 295.1810, found 295.1842

5.1.1.14. (S)-1-(3-Phenylpropyl)-3-(1,2,3,4-tetrahydronaphthalen-1-yl)urea (8h(S)). Yield 84 %; White solid; mp 133-135 °C; IR (neat): 3315, 2998, 2940, 1621, 1571, 1498, 1450 cm^{-1}; ^{1}H-NMR (CDCl$_3$) δ 1.74-1.89 (m, 6H), 1.97-2.04 (m, 1H), 2.65 (t, J = 7.80 Hz, 2H), 2.73-2.76 (m, 2H), 3.18 (t, J = 7.20 Hz, 2H), 4.50-4.60 (bs, 1H), 4.90-4.95 (m, 1H), 7.06-7.31 (m, 9H); ^{13}C-NMR (CDCl$_3$) δ 19.92, 29.19, 30.68, 31.44, 33.05, 40.30, 48.89, 126.03, 126.25, 127.28, 128.34, 128.48, 128.61, 129.12, 136.94, 137.50, 141.23, 157.80; HRMS Calcd for C$_{20}$H$_{24}$N$_2$O m/z [M+H] 309.1967, found 309.2000

5.1.1.15. (R)-1-(3-Phenylpropyl)-3-(1,2,3,4-tetrahydronaphthalen-1-yl)urea (8h(R)). Yield 81 %; White solid; mp 133-135 °C; IR (neat): 3315, 2999, 2942, 1621, 1571, 1498, 1450 cm^{-1}; ^{1}H-NMR (CDCl$_3$) δ 1.74-1.88 (m, 6H), 1.99-2.04 (m, 1H), 2.65 (t, J = 7.80 Hz, 2H), 2.70-2.81 (m, 2H), 3.19 (t, J = 7.20 Hz, 2H), 4.60-4.75 (bs, 1H), 4.92-4.94 (m, 1H), 7.07-7.31 (m, 9H); ^{13}C-

NMR (CDCl$_3$) δ 19.92, 29.19, 30.68, 31.44, 33.05, 40.30, 48.89, 126.03, 126.25, 127.28, 128.34, 128.48, 128.61, 129.12, 136.94, 137.50, 141.23, 157.80; HRMS Calcd for C$_{20}$H$_{24}$N$_2$O *m/z* [M+H] 309.1967, found 309.1999

*5.1.1.16. (S)-2-Phenyl-N-(3-phenylpropyl)pyrrolidine-1-carboxamide (**8i(S)**).* Yield 82 %; Yellow oil; IR (neat): 3335, 3025, 2864, 1628, 1527, 1494, 1346 cm^{-1}; ^{1}H-NMR (CDCl$_3$) δ 1.60-1.67 (m, 2H), 1.82-194 (m, 3H), 2.35-2.42 (m, 3H), 3.04-3.11 (m, 1H), 3.15-3.22 (m, 1H), 3.63-3.72 (m, 2H), 4.01 (bs, 1H), 4.64-4.67 (m, 1H), 7.01 (d, *J* = 7.60 Hz, 2H), 7.13-7.37 (m, 8H); ^{13}C-NMR (CDCl$_3$) δ 23.02, 31.58, 32.84, 36.78, 39.87, 47.27, 60.84, 125.74, 125.78, 127.57, 128.33, 128.34, 128.97, 141.76, 143.33, 157.12; HRMS Calcd for C$_{20}$H$_{24}$N$_2$O *m/z* [M+H] 309.1967, found 309.1996

*5.1.1.17. (R)-2-Phenyl-N-(3-phenylpropyl)pyrrolidine-1-carboxamide (**8i(R)**).* Yield 86 %; Yellow oil; IR (neat): 3335, 3025, 2863, 1628, 1528, 1494, 1346 cm^{-1}; ^{1}H-NMR (CDCl$_3$) δ 1.60-1.68 (m, 2H), 1.83-1.94 (m, 3H), 2.34-2.43 (m, 3H), 3.03-3.12 (m, 1H), 3.15-3.24 (m, 1H), 3.65-3.72 (m, 2H), 4.64-4.68 (m, 1H), 7.00-7.02 (m, 2H), 7.12-7.29 (m, 6H), 7.33-7.39 (m, 2H). ^{13}C-NMR (CDCl$_3$) δ 23.11, 31.58, 32.90, 36.74, 40.10, 47.58, 61.18, 125.76, 127.65, 128.30, 128.31, 128.97, 141.63, 142.85, 156.96; HRMS Calcd for C$_{20}$H$_{24}$N$_2$O *m/z* [M+H] 309.1967, found 309.1995

*5.1.1.18. (S)-1-sec-Butyl-3-(3-phenylpropyl)urea (**8j(S)**).* Yield 83 %; White solid; mp: 86-88 °C; IR (neat): 3331, 3020, 2866, 1625, 1564, 1498, 1448, 752, 687 cm^{-1}; ^{1}H NMR (CDCl$_3$) δ 0.90 (t, *J* = 7.20 Hz, 3H), 1.10 (d, *J* = 6.60 Hz, 3H), 1.39-1.49 (m, 2H), 1.79-1.89 (m, 2H), 2.66 (t, *J* = 7.80 Hz, 2H), 3.19 (t, *J* = 7.20 Hz, 2H), 3.57-3.64 (m, 1H), 4.40-4.65 (bs, 2H), 7.16-7.23 (m, 3H), 7.26-7.32 (m, 2H); ^{13}C NMR (75 MHz, CDCl$_3$) δ 10.23, 20.72, 29.95, 31.33, 33.09, 40.45,

48.48, 126.06, 128.36, 128.51, 141.11, 158.29; HRMS Calcd for $C_{14}H_{22}N_2O$ *m/z* [M+H] 235.1810, found 235.1835

5.1.1.19. 1-sec-Butyl-3-(3-phenylpropyl)urea (8j(RS)). Yield 80 %; White solid; mp: 86-88 °C; IR (neat): 3330, 3020, 2866, 1625, 1564, 1498, 1449, 752, 687 cm^{-1}; ^{1}H NMR (CDCl$_3$) δ 0.90 (t, *J* = 7.20 Hz, 3H), 1.10 (d, *J* = 6.60 Hz, 3H), 1.38-1.46 (m, 2H), 1.79-1.89 (m, 2H), 2.66 (t, *J* = 7.80 Hz, 2H), 3.19 (t, *J* = 7.20 Hz, 2H), 3.56-3.64 (m, 1H), 7.16-7.21 (m, 3H), 7.27-7.31 (m, 2H); ^{13}C NMR (75 MHz, CDCl$_3$) δ 10.36, 20.93, 30.10, 31.67, 33.15, 40.19, 47.86, 125.96, 128.37, 128.45, 141.48, 158.36. HRMS Calcd for $C_{14}H_{22}N_2O$ *m/z* [M+H] 235.1810, found 235.1835

5.1.2. Preparation of (S)-4-(3-(3-(1-Phenylethyl)ureido)propyl)benzenesulfonamide (8k(S)) and (R)-4-(3-(3-(1-Phenylethyl)ureido)propyl)benzenesulfonamide (8k(R))

5.1.2.1. Preparation of 2,2,2-trifluoro-N-(3-phenylpropyl)acetamide (12): To a cooled solution of 3-phenylpropylamine **11** (6.20 mmol) in methylene chloride (10 mL) at 0 °C, triethylamine (9.30 mmol) was added. After 2 minutes, trifluoroacetic anhydride (9.30 mmol) was added at the same temperature and allowed to stir for 3 h at ambient temperature. The reaction was monitored by TLC. After the completion of the reaction, the reaction mixture was quenched with water and extracted using methylene chloride. The organic layer was washed with water, dried over anhydrous Na_2SO_4 and concentrated under vacuum to get the crude product **12**. Without purification, **12** was taken for the next step. Yield 82 %; White solid; ^{1}H NMR (CDCl$_3$) δ 1.89-1.99 (m, 2H), 2.69 (t, *J* = 7.40 Hz, 2H), 3.36-3.43 (m, 2H), 6.19 (bs, 1H), 7.17-7.33 (m, 5H).

5.1.2.2. Preparation of 4-(3-(2,2,2-trifluoroacetamido)propyl)benzene-1-sulfonylchloride (13): To a cooled solution of chlorosulfuric acid (2 mL) at 0 °C, compound **12** (3.33 mmol) dissolved in methylene chloride (2 mL) was added slowly and allowed to stir for 3 h to attain ambient

temperature. The reaction was monitored by TLC. After the completion of the reaction, the reaction mixture was slowly added to crushed ice with vigorous stirring. After all ice has melt down, the reaction mass was extracted using methylene chloride and concentrated. The obtained crude residue **13** was taken for the next step. Yield 65 %; Pale yellow solid; ^{1}H NMR (CDCl$_3$) δ 1.94-2.04 (m, 2H), 2.81 (t, *J* = 7.40 Hz, 2H), 3.41-3.48 (m, 2H), 6.36 (bs, 1H), 7.44 (d, *J* = 8.40 Hz, 2H), 7.98 (d, *J* = 8.40 Hz, 2H).

*5.1.2.3. Preparation of 2,2,2-trifluoro-N-(3-(4-sulfamoylphenyl)propyl)acetamide (**14**):* To a solution of **13** (2.66 mmol) in methylene chloride (10 mL), ammonia gas was passed for a period of 30 minutes. The resulting precipitate was filtered, washed with water and dried to obtain **14.** Yield 85 %; White solid; ^{1}H NMR (DMSO-*d$_6$*) δ 1.76-1.86 (m, 2H), 2.66 (t, *J* = 7.40 Hz, 2H), 3.17-3.23 (m, 2H), 7.28 (s, 2H), 7.40 (d, *J* = 8.40 Hz, 2H), 7.74 (d, *J* = 8.40 Hz, 2H), 9.46 (bs, 1H).

*5.1.2.4. Preparation 4-(3-aminopropyl)benzenesulfonamide (**15**):* To a solution of **14** (1.20 mmol) dissolved in methanol : water mixture (1:1, 10 mL), potassium carbonate (2.40 mmol) was added and stirred at ambient temperature for 10 h. The completion of the reaction was monitored by TLC. The reaction mixture was evaporated under vacuum to obtain white solid. The resulting solid was dissolved in methanol (20 mL) and the residue was filtered. The filterate was evaporated to get the amine **15** which was used for the next step. Yield 80 %; White solid; ^{1}H NMR (D$_2$O) δ 1.75-1.82 (m, 2H), 2.63 (t, *J* = 7.40 Hz, 2H), 2.70-2.75 (m, 2H), 7.39 (d, *J* = 8.40 Hz, 2H), 7.76 (d, *J* = 8.40 Hz, 2H).

*5.1.2.5. Preparation of ureas **8k(S)** and **8k(R)**:* To a cooled solution of triphosgene (0.29 mmol) in THF at 0 °C, a mixture of amine **9** (0.88 mmol) and *N,N*-diisopropylethylamine (1.76 mmol) was added. The reaction mixture was stirred at the same temperature for 30 minutes and then the

amine **15** (0.88 mmol) was added. The reaction mixture was slowly allowed to attain ambient temperature and further stirred for 8 h. After the completion of the reaction, water was added and the reaction mixture was extracted using ethyl acetate. The organic layer was dried over anhydrous Na_2SO_4 and evaporated under reduced pressure. The crude mixture was subjected to column chromatography to obtain the **8k(*S*)** *and* **8k(*R*)**.

5.1.2.6. (S)-4-(3-(3-(1-Phenylethyl)ureido)propyl)benzenesulfonamide (8k(S)). Yield 62 %; White solid; mp: 164-166 °C; IR (neat): 3340, 3016, 2969, 1623, 1570, 1452, 1338, 1323, 1160 cm^{-1}; ^{1}H NMR (DMSO-*d₆*) δ 1.30 (d, *J* = 6.90 Hz, 3H), 1.61-1.71 (m, 2H), 2.61 (d, *J* = 7.80 Hz, 2H), 2.94-3.01 (m, 2H), 4.68-4.77 (m, 1H), 5.84-5.88 (m, 1H), 6.27 (d, *J* = 8.10 Hz, 1H), 7.17-7.31 (m, 7H), 7.36 (d, *J* = 8.40 Hz, 2H), 7.72 (d, *J* = 8.40 Hz, 2H); ^{13}C NMR (DMSO-*d₆*) δ 23.11, 31.33, 32.06, 38.53, 48.46, 125.55, 125.60, 126.22, 127.99, 128.51, 141.59, 145.69, 145.93, 157.18; HRMS Calcd for $C_{18}H_{23}N_3O_3S$ *m/z* [M+H] 362.1538, found 362.1575

5.1.2.7. (R)-4-(3-(3-(1-Phenylethyl)ureido)propyl)benzenesulfonamide (8k(R)). Yield 65 %; White solid; mp: 164-166 °C; IR (neat): 3340, 3015, 2969, 1623, 1570, 1452, 1338, 1322, 1160 cm^{-1}; ^{1}H NMR (DMSO-*d₆*) δ 1.31 (d, *J* = 6.90 Hz, 3H), 1.62-1.72 (m, 2H), 2.61 (d, *J* = 7.80 Hz, 2H), 2.95-3.02 (m, 2H), 4.68-4.78 (m, 1H), 5.82-5.84 (m, 1H), 6.23 (d, *J* = 8.10 Hz, 1H), 7.17-7.31 (m, 7H), 7.35 (d, *J* = 8.40 Hz, 2H), 7.72 (d, *J* = 8.40 Hz, 2H). ^{13}C NMR (DMSO-*d₆*) δ 23.18, 31.39, 32.09, 38.55, 48.49, 125.59, 125.64, 126.27, 128.04, 128.56, 141.61, 145.74, 145.97, 157.21; HRMS Calcd for $C_{18}H_{23}N_3O_3S$ *m/z* [M+H] 362.1538, found 362.1573

6. Biology

6.1. Evaluation of sEH inhibition with LC-MS/MS method

sEH inhibition was determined using an LC-MS/MS method of Lee *et al* [37]. The physiological substrate 14,15-EET (25 μM) was incubated at 30°C with various concentrations of test

compound and 0.1 µg/mL sEH in 25 mM bis-Tris-HCl buffer (pH = 7.0) containing 0.1 mg/mL of BSA in a total volume of 200 µL. The reactions were terminated after 20 min by the addition of 200 µL of methanol containing 200 nM 9,10-DiHOME as an internal standard. Following centrifugation (13,000 rpm for 10 min), the supernatant was used for LC-MS/MS analysis. The enzyme inhibition parameter IC_{50} was calculated by fitting the Hill equation to the data using nonlinear regression (least squares best fit modeling) of the plot of percentage control activity versus concentration of the test inhibitors using GraphPad Prism 5.0 (GraphPad Software Inc., San Diego, CA).

The LC-MS/MS experiments were performed using a Prominence[TM] UFLC system (Shimadzu, Japan) coupled with an API3200QTRAP[TM] LC-MS/MS system (Applied Biosystems, Foster City, CA) equipped with a Turbo V IonSpraysource[TM] operated in negative-ion mode. The sample injection volume was 10 µL, and the separation was performed on a XTerra[TM] MS C18 C18 column (2.1 × 150 mm, 5 μm; Waters, Milford, MA, USA) with a SecuityGuard[TM] C18 guard column (2.0 × 4.0 mm i.d.; Phenomenex) maintained at 30°C. The mobile phase consisted of deionized water (A) and acetonitrile (B). A linear gradient of the two solvents was used: start at 70 % A and hold for 0.1 min, ramp to 40 % A to 0.5 min and hold until 3 min, and ramp to 10 % A to 6 min and hold for 1 min. The flow rate was set at 0.4 mL/min, and the overall chromatographic run time was 7 min. The retention times for 14,15-DHET and the internal standard (9,10-DiHOME) were 4.4 and 4.3 min, respectively. The auto-sampler compartment was maintained at 10°C throughout the analysis. Ion source conditions for 14,15-DHET and 9,10-DiHOME were set as follows: CUR = 20, CAD = Medium, IS = −4500, TEM = 600, GS1 = 50, and GS2 = 50. Quadrupoles Q1 and Q3 were set on unit resolution. The samples were analyzed with multiple reaction monitoring. The monitoring ions were m/z 337→207 for 14,15-

DHET and m/z 313→201 for 9,10-DiHOME. In this study, the limit of detection and limit of quantification values were 1.4 and 4.2 pg/mL with the signal-to-noise ratios over 2 and 10, respectively.

6.2. HPLC method for evaluating mEH inhibition

mEH inhibition was determined using an HPLC method of Lee *et al* [37]. The substrate styrene oxide (25 µM) was incubated with 10 µM test compound and pooled human liver microsomes (0.2 mg/mL) in 0.1 M Tris-HCl (pH 9.0) in a total volume of 200 µL. Valpromide was used as a positive mEH inhibitor. The reactions were incubated at 37°C for 10 min and terminated by the addition of 200 µL of n-hexane. Following centrifugation (13,000 rpm, 10 min), the supernatant was used for UV-HPLC analysis. The mEH activity of each sample was calculated according to the amount of styrene glycol produced and is expressed as the percentage of the control activity.

The determination of styrene glycol was performed using a Shimadzu LC-10AD (Kyoto, Japan) equipped with a UV detector (Shimadzu SPD-20A), controller (Shimadzu SIL-20AC), and column oven (Shimadzu CTO-10AS). A Phenomenex Luna C18 column (150×4.5 mm, 5 µm) was used at 30°C with 40% methanol as the mobile phase, at a flow rate of 1.5 mL/min. Standard and extracted samples of 10 µL were injected onto the column. The UV absorbance was monitored at 208 nm.

7. Binding Model Prediction of sEH Inhibitors

The crystal structure of human soluble epoxide hydrolase from Protein Data Bank (PDB code; 4OCZ [18], a complex with the 1-(1-isobutylpiperidin-4-yl)-3-(4-(trifluoromethyl)-phenyl)urea) was used for docking simulation. The sEH inhibitors were built using a Maestro build panel in the Schrodinger Package. The compounds were minimized using the Impact module of Maestro in the Schrödinger Suite Program. The starting coordinate of the human peroxidase was further

modified for binding model prediction. The protein structure was minimized using the Protein Preparation Wizard by applying an OPLS-5 force field [38]. After complete preparation of the ligands and protein for docking, receptor-grid files were generated. Ligand docking into the active site of human sEH was carried out using the Schrödinger docking program, Glide [39]. The energy minimized sEH inhibitors were docked into the prepared receptor grid. The best-docking models of sEH inhibitors with the lowest Glide docking score were adopted as the binding conformation.

ACKNOWLEDGMENT

REFERENCES

[1] A.A. Spector, Arachidonic acid cytochrome P450 epoxygenase pathway, J. Lipid Res. 50 (2009) 52-56.

[2] M.F. Moghaddam, D.F. Grant, J.M. Cheek, J.F. Greene, K.C. Williamson, B.D. Hammock, Bioactivation of leukotoxins to their toxic diols by epoxide hydrolase, Nat. Med. 3 (1997) 562-566.

[3] M.A. Carroll, J.C. McGiff, A new class of lipid mediators: Cytochrome P450 arachidonate metabolites, Thorax. 55 (2000) 13-16.

[4] J.H. Capdevila, J.R. Falck, R.C. Harris, Cytochrome P450 and arachidonic acid bioactivation: Molecular and functional properties on the arachidonate monooxygenase, J. Lipid Res. 41 (2000) 163-181.

[5] Z. Yu, F. Xu, L.M. Huse, C. Morisseau, A.J. Draper, J.W. Newman, C. Parker, L. Graham, M.M. Engler, B.D. Hammock, D.C. Zeldin, D.L. Kroetz, Soluble epoxide hydrolase regulates hydrolysis of vasoactive epoxyeicosatrienoic acids, Circ. Res. 87 (2000) 992-998.

[6] J.D. Imig, X. Zhao, J.H. Capdevila, C. Morisseau, B.D. Hammock, Soluble epoxide hydrolase inhibition lowers arterial blood pressure in angiotensin II hypertension, Hypertension 39 (2002) 690-694.

[7] X. Zhao, T. Yamamoto, J.W. Newman, I.H. Kim, T. Watanabe, B.D. Hammock, J. Stewart, J.S. Pollock, D.M. Pollock, J.D. Imig, Soluble epoxide hydrolase inhibition protects the kidney from hypertension-induced damage, J. Am. Soc. Nephrol. 15 (2004), 1244-1253.

[8] J.D. Imig, X. Zhao, C.Z. Zaharis, J.J. Olearczyk, D.M. Pollock, J.W. Newman, I.H. Kim, T. Watanabe, B.D. Hammock, An orally active epoxide hydrolase inhibitor lowers blood pressure and provides renal protection in salt-sensitive hypertension, Hypertension 46 (2005) 975–981.

[9] O. Jung, R.P. Brandes, I.H. Kim, F. Schweda, R. Schmidt, B.D. Hammock, R. Busse, I. Fleming, Soluble epoxide hydrolase is a main effector of angiotensin II-induced hypertension, Hypertension 45 (2005) 759–765.

[10] Jr. J.P. Marino, Soluble epoxide hydrolase, a target with multiple opportunities for cardiovascular drug discovery, Curr. Top. Med. Chem. 9 (2009) 452–463.

[11] G.J. Gross, K. Nithipatikom, Soluble epoxide hydrolase: A new target for cardioprotection, Curr. Opin. Investig. Drugs 10 (2009), 253–258.

[12] N. Chiamvimonvat, C.M. Ho, H.J. Tsai, B.D. Hammock, The soluble epoxide hydrolase as a pharmaceutical target for hypertension, J. Cardiovasc. Pharmacol. 50 (2007) 225–237.

[13] J.D. Imig, Cardiovascular therapeutic aspects of soluble epoxide hydrolase inhibitors. Cardiovasc. Drug Rev. 24 (2006) 169–188.

[14] H.C. Shen, B.D. Hammock, Discovery of inhibitors of soluble epoxide hydrolase: A target with multiple potential therapeutic indications, J. Med. Chem. 55 (2012) 1789–1808.

[15] T.R. Harris, A. Bettaieb, S. Kodani, H. Dong, R. Myers, N. Chiamvimonvat, F.G. Haj, B.D. Hammock, Inhibition of soluble epoxide hydrolase attenuates hepatic fibrosis and endoplasmic reticulum stress induced by carbon tetrachloride in mice, Toxicol. Appl. Pharmacol. 286 (2015) 102-111.

[16] F.A. Fitzpatrick, M.D. Ennis, M.E. Baze, M.A. Wynalda, J.E. McGee, W.F. Liggett, Inhibition of cyclooxygenase activity and platelet aggregation by epoxyeicosatrienoic acids, J. Biol. Chem. 261 (1986) 15334–15338.

[17] F. Krotz, T. Riexinger, M.A. Buerkle, K. Nithipatikom, T. Gloe, H.Y. Sohn, W.B. Campbell, U. Pohl, Membrane potential-dependent inhibition of platelet adhesion to endothelial cells by epoxyeicosatrienoic acids, Arterioscler. Thromb. Vasc. Biol. 24 (2004) 595–600.

[18] K.S.S. Lee, J-Y. Liu, K.M. Wagner, S. Pakhomova, H. Dong, C. Morisseau, S.H. Fu, J. Yang, P. Wang, A. Ulu, C.A. Mate, L.V. Nguyen, S.H. Hwang, M.L. Edin, A.A. Mara, H. Wulff, M.E. Newcomer, D.C. Zeldin, B.D. Hammock, Optimized inhibitors of soluble epoxide hydrolase improve in vitro target residence time and in vivo efficacy, J. Med. Chem. 57 (2014) 7016-7030.

[19] S. Norwood, J. Liao, B.D. Hammock, G.-Y. Yang, Epoxyeicosatrienoic acids and soluble epoxide hydrolase: potential therapeutic targets for inflammation and its induced carcinogenesis, Am. J. Transl. Res. 2 (2010) 447-457.

[20] G. Zhang, S. Kodani, B.D. Hammock, Stabilized epoxygenated fatty acids regulate inflammation, pain, angiogenesis and cancer, Prog. Lipid. Res. 53 (2014) 108-123.

[21] I.-H. Kim, F.R. Heirtzler, C. Morisseau, K. Nishi, H.-J. Tsai, B.D. Hammock, Optimization of amide-based inhibitors of soluble epoxide hydrolase with improved water solubility, J. Med. Chem. 48 (2005) 3621-3629.

[22] I-H. Kim, I-H. Lee, H. Nishiwaki, B.D. Hammock, K. Nishi, Structure–activity relationships of substituted oxyoxalamides as inhibitors of the human soluble epoxide hydrolase, Bioorg. Med. Chem. 22 (2014) 1163-1175.

[23] H.C. Shen, F.-X. Ding, Q. Deng, S. Xu, X. Tong, X. Zhang, Y. Chen, G. Zhou, L.-Y. Pai, M. Alonso-Galicia, S. Roy, B. Zhang, J.R. Tata, J.P. Berger, S.L. Colletti, A strategy of employing aminoheterocycles as amide mimics to identify novel, potent and bioavailable soluble epoxide hydrolase inhibitors, Bioorg. Med. Chem. Lett. 19 (2009) 5716-5721.

[24] L. Tang, W.-H. Ma, Y.-L. Ma, S.-R. Ban, X.-E. Feng, Q.-S. Li, Synthesis and biological activity of 4-substituted benzoxazolone derivatives as a new class of sEH inhibitors with high anti-inflammatory activity in vivo, Bioorg. Med. Chem. Lett. 23 (2013) 2380-2383.

[25] E.R. Zavareh, M. Hedayati , L.H. Rad, S. Shahhosseini, M. Faizi, S. A. Tabatabai, Design, synthesis and biological evaluation of 4-benzamidobenzoic acid hydrazide derivatives as novel soluble epoxide hydrolase inhibitors, Iran. J. Pharm. Res. 13 (2004) 51-59.

[26] Y. Amano, E. Tanabe, T. Yamaguchi, Identification of *N*-ethylmethylamine as a novel scaffold for inhibitors of soluble epoxide hydrolase by crystallographic fragment screening, Bioorg. Med. Chem. 23 (2015) 2310-2317.

[27] S.H. Hwang, H.-J. Tsai, J.-Y. Liu, C. Morisseau, B.D. Hammock, Orally bioavailable potent soluble epoxide hydrolase inhibitors, J. Med. Chem. 50 (2007) 3825-3840.

[28] I.-H. Kim, H.-J. Tsai, K. Nishi, T. Kasagami, C. Morisseau, B.D. Hammock, 1,3-Disubstituted ureas functionalized with ether groups are potent inhibitors of the soluble epoxide hydrolase with improved pharmacokinetic properties, J. Med. Chem. 50 (2007) 5217-5226.

[29] S.-X. Huang, B. Cao, C. Morisseau, Y. Jin, B.D. Hammock, Y.-Q. Long, Structure-based optimization of the piperazino-containing 1,3-disubstituted ureas affording sub-nanomolar inhibitors of soluble epoxide hydrolase, Med. Chem. Comm. 3 (2012) 379-384.

[30] V. Burmistrov, C. Morisseau, K.S.S. Lee, D.S. Shihadih, T.R. Harris, G.M. Butov, B.D. Hammock, Symmetric adamantyl-diureas as soluble epoxide hydrolase inhibitors, Bioorg. Med. Chem. Lett. 24 (2014) 2193-2197.

[31] G.A. Gomez, C. Morisseau, B.D. Hammock, D.W. Christianson, Human soluble epoxide hydrolase: Structural basis of inhibition by 4-(3- cyclohexylureido)-carboxylic acids, Protein Sci. 15 (2006) 58-64.

[32] C. Morisseau, M.H. Goodrow, D. Dowdy, J. Zheng, J.F. Greene, J.R. Sanborn, B.D. Hammock, Potent urea and carbamate inhibitors of soluble epoxide hydrolases. Proc. Natl. Acad. Sci. USA. 96 (1999) 8849-8854.

[33] R. Lonsdale, S. Hoyle, D.T. Grey, L. Ridder, A.J. Mulholland, Determinants of Reactivity and Selectivity in Soluble Epoxide Hydrolase from Quantum Mechanics/Molecular Mechanics Modeling, Biochemistry 51 (2012) 1774-1786.

[34] C. Chiappe, C.D. Palese, Stereo- and enantioselectivity of the soluble epoxide hydrolase catalyzed hydrolysis of ($\pm$) cis-dialkyl substituted oxiranes, Tetrahedron, 55(1999) 11589-11594.

[35] D.C. Zeldin, J. Kobayashi, J.R. Falck, B.S. Winder, B.D. Hammock, J.R. Snapper, J.H. Capdevila, Regio- and enantiofacial selectivity of epoxyeicosatrienoic acid hydration by cytosolic epoxide hydrolase, J. Biol. Chem. 268 (1993) 6402-6407.

[36] D.D. Perrin, W.L.F. Armarego, D.R. Perrin, Purification of Laboratory Chemicals, second ed., Pergamon Press, Oxford, England, 1982.

[37] G.H. Lee, S.J. Oh, S.Y. Lee, J.Y. Lee, J.Y. Ma, Y.H. Kim, S.K. Kim, Discovery of soluble epoxide hydrolase inhibitors from natural products, Food Chem. Toxicol. 64 (2014) 225-230.

[38] Schrodinger Release 2015-1, Schrodinger Suite 2015-1 Protein Preparation Wizard, Epik version 3.1, Schrodinger, LLC, New York, NY, 2015, Impact version 6.6, Schrödinger, LLC, New York, NY, 2015, Prime version 3.9, Schrodinger, LLC, New York, NY, 2015.

[39] Small-Molecule Drug Discovery Suite 2015-1, Glide, version 6.6, Schrödinger, LLC, New York, NY, 2015.

Highlights

➢ Enantioselectivity in 1-(α-alkyl-α-phenylmethyl)-3-(3-phenylpropyl)ureas for the inhibition of soluble epoxide hydrolase (sEH) was first time discovered.

➢ The *S*-isomer of **8e** showed 125 fold more active than its *R*-isomer.

➢ Restriction of the free rotation of two α-groups with indan-1-yl or 1,2,3,4-tetrahydronaphthalen-1-yl moiety abolishes the selectivity between the enantiomers.

➢ These urea analogs are specific inhibitor of sEH without inhibition of mEH.